

Impact of the phonon coupling on the photon strength function

O. Achakovskiy and A. Avdeenkov

Institute for Physics and Power Engineering, 249033 Obninsk, Russia

S. Goriely

Institut d'Astronomie et d'Astrophysique, ULB, CP 226, B-1050 Brussels, Belgium

S. Kamedzhiev*

Institute for Nuclear Power Engineering NRNU MEPHI, 249040 Obninsk, Russia

S. Krewald

Institut für Kernphysik, Forschungszentrum Jülich, D-52425 Jülich, Germany

The pygmy dipole resonance and photon strength function in stable and unstable Ni and Sn isotopes are calculated within the microscopic self-consistent version of the extended theory of finite fermi systems which includes phonon coupling effects. The Skyrme force SLy4 is used. A pygmy dipole resonance in ^{72}Ni is predicted at the mean energy of 12.4 MeV exhausting 25.7% of the total energy-weighted sum rule. The microscopically obtained photon E1 strength functions are compared with available experimental data and used to calculate nuclear reaction properties. Average radiative widths and radiative neutron capture cross sections have been calculated taking the phonon coupling into account as well as the uncertainties caused by various microscopic level density models. In all three quantities considered, the contribution of phonon coupling turned out to be significant and is found necessary to explain available experimental data.

PACS numbers: 24.10.-i, 24.60.Dr, 24.30.Cz, 21.60.Jz

The photon strength function (PSF) is a quantity of fundamental importance in the description of nuclear reactions involving electromagnetic excitations or de-excitations. In particular, the PSF is known to significantly affect the radiative neutron capture cross section for incident neutrons in the keV region, a range of energies of particular relevance in astrophysical [1, 2] as well as nuclear engineering [3] applications. Traditionally, the de-excitation PSF has been parametrized phenomenologically on the basis of simple Lorentzian-type functions [4–6] and associated with the photoabsorption strength function on the basis of the Brink hypothesis [4] which assumes that on each excited state, it is possible to build a giant dipole resonance (GDR) equivalent to the one observed in the reverse photoabsorption process. For the last decades, an important effort has been devoted to the determination of the low-lying strength, i.e. the tail of the GDR. This low-lying strength, in particular below the neutron threshold, is known to be of relevance in radiative neutron cross section. The presence of any extra strength with respect to the tail of the GDR, this so-called pygmy dipole resonance (PDR), has been found to exhaust typically about 1-2% of the Energy Weighted Sum Rule (EWSR) but also to affect significantly the radiative neutron capture cross section and potentially the nucleosynthesis of neutron-rich nuclei by the r-process [7]. Recent experiments [8–11] have provided additional information about the PDR and PSF structure that clearly

cannot be explained by standard phenomenological approaches. It was also shown that in neutron-rich nuclei, the strength could be significantly more important than in nuclei close to the valley of β -stability [1, 2]. For all these reasons, there has been a growing interest in the investigation of the PDR energy region both by the low-energy nuclear physics community [8, 12] and within the field of nuclear data [1, 2, 5, 6].

Since the presence, strength and structures of a PDR cannot be predicted within the Lorentzian-type approach, microscopic models need to be applied. Mean-field approaches using effective nucleon interactions, such as the Hartree-Fock Bogoliubov (HFB) method and the quasi-particle random-phase approximation (QRPA) allow for systematic self-consistent studies of the E1 strength functions. Provided damping and deformation corrections are included phenomenologically on top of the HFB+QRPA strength, such methods have proven their capacity to reproduce fairly well the photoabsorption data in the vicinity of the GDR. However, as discussed below and as confirmed by recent experiments (see for example [10]), the HFB+QRPA approach fails to reproduce fine structures and needs to be renormalized on GDR data. To be exact, it should be complemented by the effect describing the interaction between the single-particle and low-lying collective phonon degrees of freedom, known as the phonon coupling (PC) [13–16]. Such an interaction was originally considered in the quasiparticle-phonon model [16, 17].

In this work, to go beyond the HFB+QRPA method, we use the self-consistent version of the extended theory of finite fermi systems (ETFFS) [13] in the quasi-

*kaev@obninsk.com

particle time blocking approximation (QTBA) [18]. Our ETFFS(QTBA) method, or simply QTBA, includes self-consistently the QRPA and PC effects and the single-particle continuum in a discrete form. Details of the method can be found in Ref. [14]. The method also allows us to investigate the impact of the PC on nuclear reactions in both stable and unstable nuclei. To do so, we calculate the microscopic PSFs in different Sn and Ni isotopes and use them to estimate the impact of the PC on radiative neutron capture cross section as well as on the average radiative widths on the basis of modern nuclear reaction codes like EMPIRE [19] and TALYS [20].

The strength function $S(\omega) = dB(E1)/dE$ [13, 14], related to the PSF $f(E1)$ by $f(E1, \omega)[\text{MeV}^{-3}] = 3.487 \cdot 10^{-7} S(\omega)[\text{fm}^2 \text{MeV}^{-1}]$, is calculated by the QTBA method [13, 18] on the basis of the well-known SLy4 Skyrme force [21]. The ground state is calculated within the HFB method using the spherical code HFBRAD [22]. The residual interaction for the (Q)RPA and QTBA calculations is derived as the second derivative of the Skyrme functional. In all our calculations we use a smoothing parameter of 200 keV which effectively accounts for correlations beyond the considered PC. Such a choice guarantees a proper description of all three characteristics of giant resonances, including the width [13], and also corresponds to the experimental resolution of reference in the present work [9].

In Fig. 1, the E1 PSF for specific even-even Sn and Ni isotopes is compared with experimental data obtained with the Oslo method [9] for Sn isotopes as well as the phenomenological Enhanced Generalized Lorentzian (EGLO) model [5]. It can be seen that *i*) in contrast to phenomenological models, the structure patterns caused by both the QRPA and PC effects are pronounced in both Sn and Ni isotopes. Physically, the PC structures are caused by the PC poles at $\omega = \epsilon_1 - \epsilon_2 - \omega_s$ or $\omega = E_1 + E_2 - \omega_s$, where $\epsilon_1, E_1, \omega_s$ are single-particle, quasi-particle and phonon energies, respectively. Such a PC effect is seen to become significant above 3 MeV and below typically 9–10 MeV; *ii*) for ^{118}Sn and ^{122}Sn isotopes, a reasonable agreement with experiment is obtained within the QRPA below typically 5 MeV. For all three Sn isotopes, at $E > 5$ MeV, the inclusion of PC effects is needed to reconcile predictions with experiment [9]; *iii*) globally, the EGLO description of the experimental data is noticeably worse than the one achieved by the QTBA.

In Table I, the integral parameters (mean energy E and fraction of EWSR exhausted) of the PDR are given for three Ni isotopes, as predicted by both QRPA and QTBA (QRPA+PC) models. To compare results in these three nuclei, a 6 MeV energy interval, which corresponds to the one where the PDR was observed in ^{68}Ni , is considered. In this interval, the PDR characteristics have been approximated, as usually, with a Lorentz curve by fitting the three moments of the theoretical curves [13]. For ^{68}Ni , a good agreement is obtained with experimental data of $E \simeq 11$ MeV and about 5% of the total EWSR

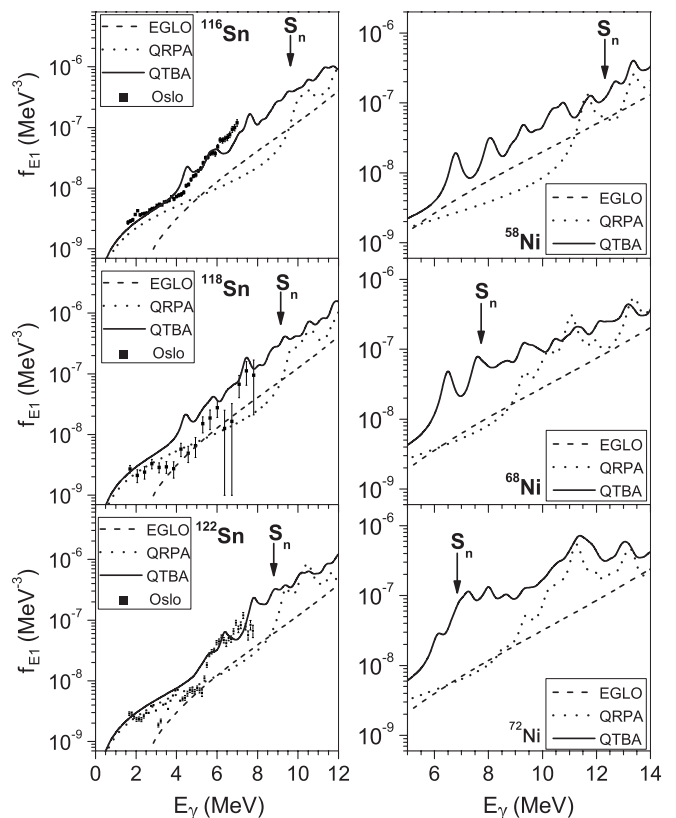


FIG. 1: E1 PSF for $^{116,118,122}\text{Sn}$ and for $^{58,68,72}\text{Ni}$ in the low-energy PDR energy region. Dotted lines correspond to the self-consistent QRPA, full lines to the QTBA (including PC), and dashed lines to the EGLO model [5]. For Sn isotopes, experimental data are taken from [9].

[23]. A similar calculation was performed for ^{68}Ni [24] using the relativistic QTBA, with two phonon contributions additionally taking into account. For the PDR characteristics in ^{72}Ni in the (8-14) MeV range, we obtain a mean energy $E = 12.4$ MeV, width $\Gamma = 3.5$ MeV and a large strength of 25.7% of the EWSR. It should be noted that the main contribution to the ^{72}Ni PDR is found in the (10-14) MeV interval which exhausts 13.9% of the EWSR for QRPA and 23.2% for QTBA. In this interval, two maxima can be observed (Fig 1). For this reason, the strength in the (10-14) MeV dominates and is globally equivalent to the one in (8-14) MeV. A large PC contribution to the PDR strength is found in all isotopes (Table I).

In Figs. 2 and 3 we present the radiative neutron capture cross sections estimated with the Hauser-Feshbach reaction code TALYS [20] on the basis of the newly determined gamma-strength function. Similar results are obtained if use is made of the EMPIRE reaction code [19]. The calculations were performed with different nuclear level density (NLD) models, including the backshifted Fermi gas model [25], the Generalized Superfluid model (GSM) [5] and the HFB plus Combinatorial model [26, 27]. The NLD is constrained by experimental neu-

TABLE I: Integral characteristics of the PDR (centroid energy E in MeV and fraction of the EWSR) in Ni isotopes calculated in the (8-14) MeV interval for ^{58}Ni , ^{72}Ni and (7-13) MeV interval for ^{68}Ni (see text for details).

Nuclei	QRPA		QTBA	
	E	%	E	%
^{58}Ni	13.3	6.0	14.0	11.7
^{68}Ni	11.0	4.9	10.8	8.7
^{72}Ni	12.4	14.7	12.4	25.7

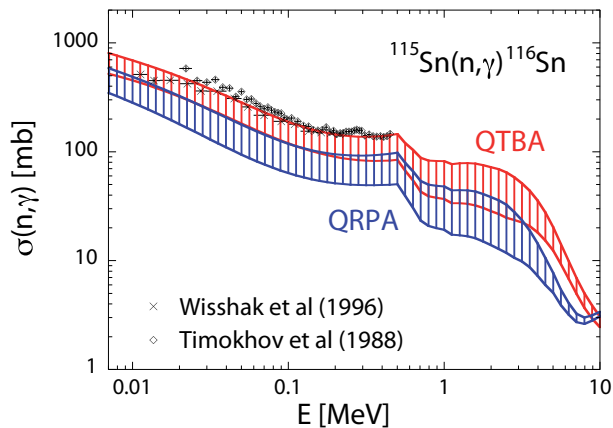


FIG. 2: (Color online) $^{115}\text{Sn}(n,\gamma)^{116}\text{Sn}$ cross section calculated with the QRPA (blue) and QTBA (red) PSF. The uncertainty bands depict the uncertainties affecting the NLD predictions [5, 25–27]. Experimental cross sections are taken from Refs. [28, 29].

tron spacings and low-lying states, whenever available [6]. As seen in Figs. 2-3, the agreement with experiment is only possible when the PC is taken into account. QRPA approach clearly underestimates the strength at low energies. This deficiency is often cured by empirically shifting the QRPA strength to lower energies or broadening the distribution [1, 2].

To test the low-lying strength predicted within the various existing models, we also consider the average radiative widths of neutron resonances Γ_γ , known to be a property of importance in the description of the γ -decay from high-energy nuclear states. This quantity is used in nuclear reaction calculations, in particular, to normalize the PSF around the neutron threshold and is defined by [32]

$$\Gamma_\gamma = \sum_{I=|J-1|}^{J+1} \int_0^{S_n} \epsilon_\gamma^3 f_{E1}(\epsilon_\gamma) \frac{\rho(S_n - \epsilon_\gamma, I)}{\rho(S_n, J)} d\epsilon_\gamma, \quad (1)$$

where ρ is the NLD and J the spin of the initial state in the compound nucleus. Extended compilation of experimental data for Γ_γ can be found in Refs. [3, 5, 6]. We have calculated the Γ_γ values for 13 Sn and Ni isotopes on the basis of the EMPIRE code [19] for the 3

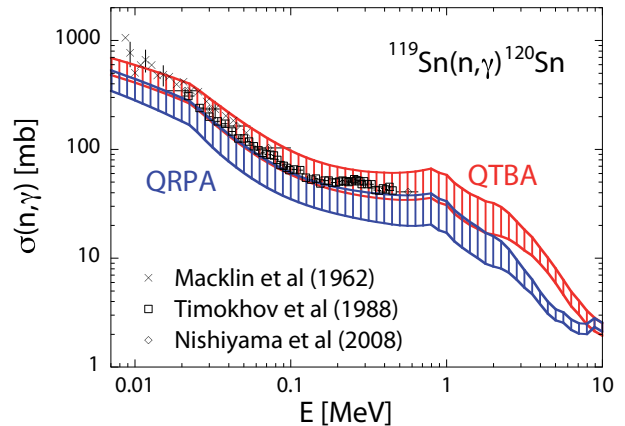


FIG. 3: (Color online) Same as Fig. 2 for $^{119}\text{Sn}(n,\gamma)^{120}\text{Sn}$. Experimental cross section are taken from Refs. [29–31]

different PSF models, namely EGLO, our SLy4+QRPA and the present QTBA, together with different NLD prescriptions, namely the GSM [5] and the microscopic HFB plus combinatorial model [26]. The predictions are compared in Table II with experimental data [3], whenever available, and with existing systematics [5, 6]. As seen in Table. II, the PC effect in stable nuclei significantly increases the QRPA contribution and improves the agreement with the systematics. Except for ^{122}Sn and ^{124}Sn , where the increase is limited, the PC leads to an enhancement of about 50 to 200%.

Our Γ_γ results for ^{118}Sn , ^{120}Sn and ^{62}Ni , for which experimental data (not systematics) exists, are of special interest. On the basis of the QTBA strength and the microscopic HFB plus combinatorial NLD [26], we obtain a good agreement with experiment for ^{62}Ni , and reasonable for ^{118}Sn and ^{120}Sn . Note that on top of the E1 strength, an M1 contribution following the recommendation of Ref. [6] is included in the calculation of Γ_γ . The M1 resonance contribution to Γ_γ has been estimated using the GSM NLD model and the standard Lorentzian parametrization [6] with a width $\Gamma = 4$ MeV (note that such a large Γ value is open to question, as discussed in Ref. [33]). Such a contribution is found to be of the order of (10-12)% of the values in the first line of Table. II for Sn isotopes and 4%, 3%, 22% and 16% for ^{58}Ni , ^{62}Ni , ^{68}Ni and ^{72}Ni , respectively. The agreement of the Γ_γ values with experiment is found to deteriorate if use is made of the EGLO or QRPA strengths, but also of the GSM NLD. One can also see that for stable nuclei, the combinatorial NLD model results are in a better agreement with the systematics [5] than those obtained with the GSM model. As far as the EGLO model is concerned, we see that similar conclusions can be drawn.

In conclusion, the microscopic E1 PSFs for 13 Sn and Ni isotopes have been calculated within the self-consistent QTBA approach which takes into account the QRPA and PC effects and uses the known SLy4 Skyrme

TABLE II: Average radiative widths Γ_γ (meV) for s-wave neutrons. For each approach (EGLO, QRPA and QTBA) two NLD models are considered: the phenomenological GSM [5] (first line) and the microscopic HFB plus combinatorial model [26] (second line). See text for details.

	^{110}Sn	^{112}Sn	^{116}Sn	^{118}Sn	^{120}Sn	^{122}Sn	^{124}Sn	^{132}Sn	^{136}Sn	^{58}Ni	^{62}Ni	^{68}Ni	^{72}Ni
EGLO	147.4	105.5	72.9	46.6	55.0	56.6	49.9	398	11.1	1096	794	166	320
	207.9	160.3	108.9	106.7	124.3	110.2	128.7	4444	295.0	2017	1841	982.2	86.4
QRPA	45.6	34.4	30.4	22.1	23.8	27.9	22.3	133	11.2	358	623	754	83.8
	71.0	49.7	44.3	40.3	43.0	50.1	68.9	4279	447.8	450.8	490.9	406.4	46.7
QTBA	93.5	65.7	46.8	33.1	34.1	35.8	27.9	148	12.3	1141	1370	392	154
	119.9	87.0	58.4	58.1	61.5	64.0	84.8	4259	509.2	1264	2117	2330	53.8
Exp. [3]				117 (20)	100 (16)						2000 (300)		
Exp. [5]				80 (20)							2200 (700)		
System.	112	109	107	106	105	104	103	85	73	2650	1300	420	320

force. They have been used to calculate the radiative neutron capture cross sections and average radiative widths of neutron resonances. A reasonable agreement with available experimental data has been obtained thanks to the PC which turns out to contribute significantly.

Our results show the necessity to include the PC effects into the theory of radiative nuclear data for low-energy nuclear physics for both stable and unstable nuclei. The QTBA method remains to be applied to the bulk of nuclei of astrophysical interest, but also to be compared with

alternative approaches which take the PC into account.

The work has been supported within the cooperation between INPE NRNU MIPHI and Institute für Kernphysik FZ Jülich. We acknowledge E. Abrosimova, expert for International Research Funding and Cooperation of the Peter Grünberg Institute/ Jülich Centre for Neutron Science, Forschungszentrum Jülich for significant help within this project. S. Ka-ev acknowledges useful discussions with Dr. V. Furman.

-
- [1] S. Goriely, E. Khan, Nucl. Phys. A **706**, 217 (2002).
[2] S. Goriely, E. Khan, V. Samyn, Nucl. Phys. A **739**, 331 (2004).
[3] S.F. Mughabghab, *Atlas of neutron Resonances, Resonance Parameters and Thermal Cross Sections Z=1-100* (Elsevier, Amsterdam, 2006)
[4] D.M. Brink, Ph.D Thesis, Oxford University (1955).
[5] T. Belgya, O. Bersillon, R. Capote et al., *Handbook for Calculations of Nuclear Reaction Data, RIPL-2*, IAEA-TECDOC-1506 (IAEA, Vienna, 2006) [<http://www-nds.iaea.org/RIPL-2/>].
[6] R. Capote et al., Nuclear Data Sheets **110**, 3107 (2009). See also <https://www-nds.iaea.org/RIPL-3>.
[7] M. Arnould, S. Goriely, K. Takahashi, Phys. Rep. **450**, 97 (2007).
[8] D. Savran, T. Aumann, A. Zilges, Prog. Part. and Nucl. Phys. **70**, 210 (2013)
[9] H.K. Toft et al., Phys. Rev. C **83**, 044320 (2011)
[10] H. Utsunomiya, et al., Phys. Rev. C **84**, 055805 (2011).
[11] R. Schwengner et al., Phys. Rev. C **87**, 024306 (2013).
[12] N. Paar, D. Vretenar, E. Khan, G. Colo, Rep. Prog. Phys. **70**, 691 (2007).
[13] S. Kamedzhiev, J. Speth, G. Tertychny, Phys. Rep. **393**, 1 (2004).
[14] A. Avdeenkov, S. Goriely, S. Kamedzhiev, S. Krewald, Phys. Rev. C **83**, 064316 (2011).
[15] S.P. Kamedzhiev, A.V. Avdeenkov, O.I. Achakovskiy, Phys. Atom. Nucl. **77**, 1303 (2014).
[16] V.G. Soloviev, Ch. Stoyanov and V.V. Voronov, Nucl. Phys. **A304**, 503 (1978).
[17] V.G. Soloviev, *Theory of complex nuclei* (Oxford: Pergamon Press, 1976).
[18] V. Tselyaev, Phys. Rev. C **75**, 024306 (2007)
[19] R. Herman, R. Capote, B.V. Carlson, P. Oblozinsky, M. Sin, A. Trkov, H. Wienke, V. Zerkin, Nucl. Data Sheets, **108** 2655 (2007).
[20] A.J. Koning and D. Rochman, Nuclear Data Sheets **113**, 2841 (2012).
[21] E. Chabanat, P. Bonche, P. Haensel, Nucl. Phys. A **635**, 231 (1998)
[22] K.Bennaceur and J. Dobaczewski, Comp. Phys. Comm, **168**, 96 (2005).
[23] O. Wieland, et al., Phys. Rev. Lett. **102**, 092502 (2009)
[24] E. Litvinova, P. Ring, V. Tselyaev, Phys. Rev. Lett. **105**, 022502 (2010).
[25] A.J. Koning, S. Hilaire, S. Goriely Nucl. Phys. A **810**, 13 (2008).
[26] S. Goriely, S. Hilaire, A.J. Koning, Phys. Rev. C **78**, 064307 (2008).
[27] S. Hilaire, M. Girod, S. Goriely, A.J. Koning, Phys. Rev. C **86**, 064317 (2012).
[28] K.Wisshak, et al., Phys. Rev. C **54**, 1451 (1996).
[29] V.M. Timokhov et al., Fiz.-Energ Institut, Obninsk Reports No.1921 (1988).
[30] R.L.Macklin, T.Inada, J.H.Gibbons, Washington AEC Office Reports, No.1041, p.30 (1962)
[31] J.Nishiyama, M.Igashira, T.Ohsaki et al., J. Nucl. Sci. Technol. (Tokyo) **45**, 352 (2008)
[32] T.S. Belanova, A.V. Ignatyuk, A.B. Pashchenko, V.I. Plyaskin, Handbook *Radiative neutron capture*, 1986
[33] S.P. Kamedzhiev, S.F. Kovalev, Phys. At. Nucl. **69**, 418 (2006).